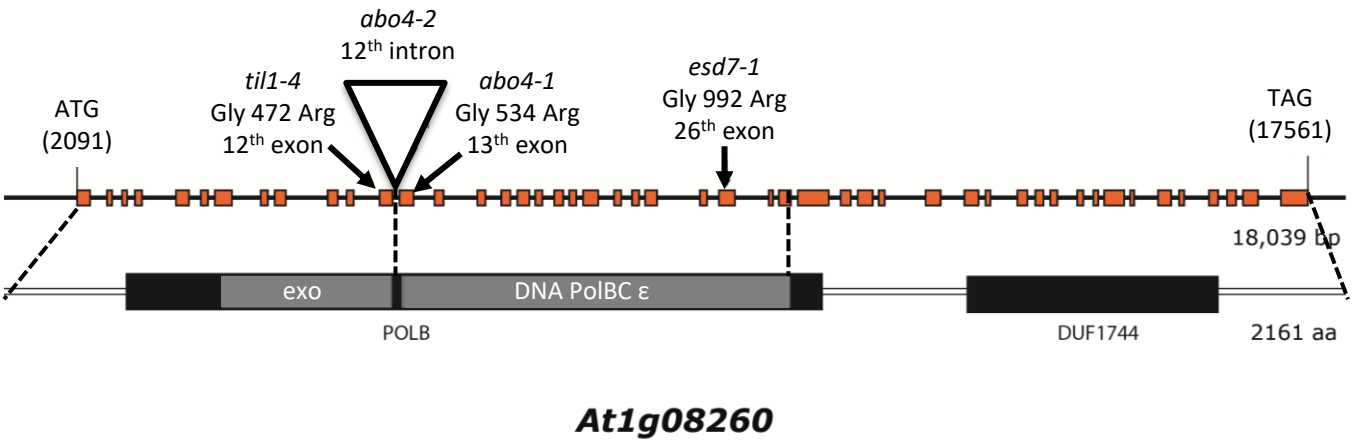

Figure S1: Positions of the mutations in *POL2A* used in this study.
Top: schematic representation of the *POL2A* gene. Orange boxes represent exons.
Bottom: schematic representation of the POL2A protein with the exonuclease (exo), DNA polymerase (PolBC) and conserved C-terminal (Domain of Unknown Function, DUF 1744) domains.

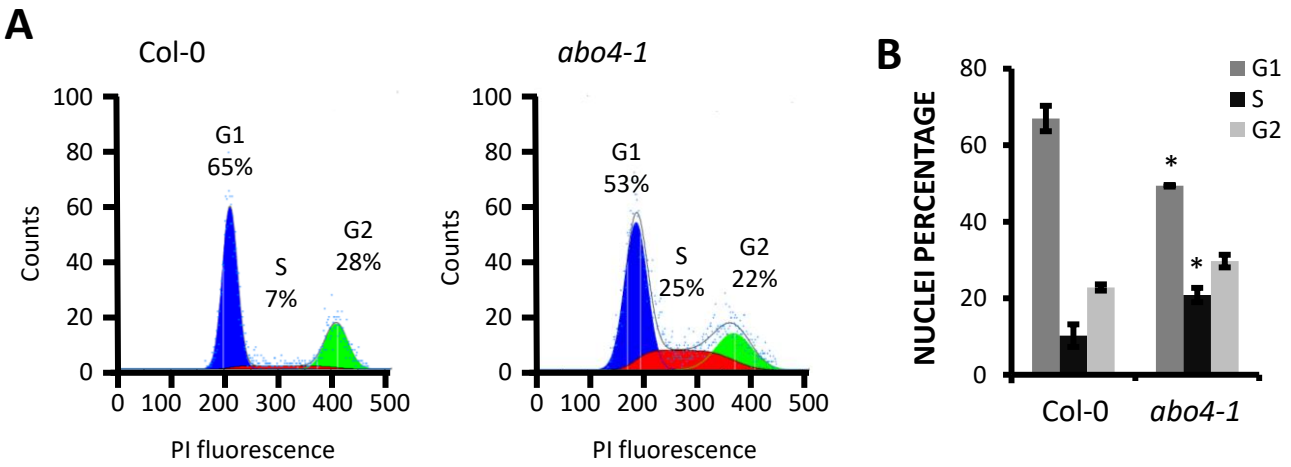

Figure S2: Cell cycle regulation is altered in *abo4-1* mutants.
A: Representative flow cytometry profiles obtained on flower buds of wild-type (Col-0) and *abo4-1* mutants. The proportion of S-phase nuclei is increased in *abo4-1*. B: average proportion of G1, S and G2 nuclei in flower buds of wild-type (Col-0) and *abo4-1* mutants. Data are average +/- s.d. from three biological replicates.

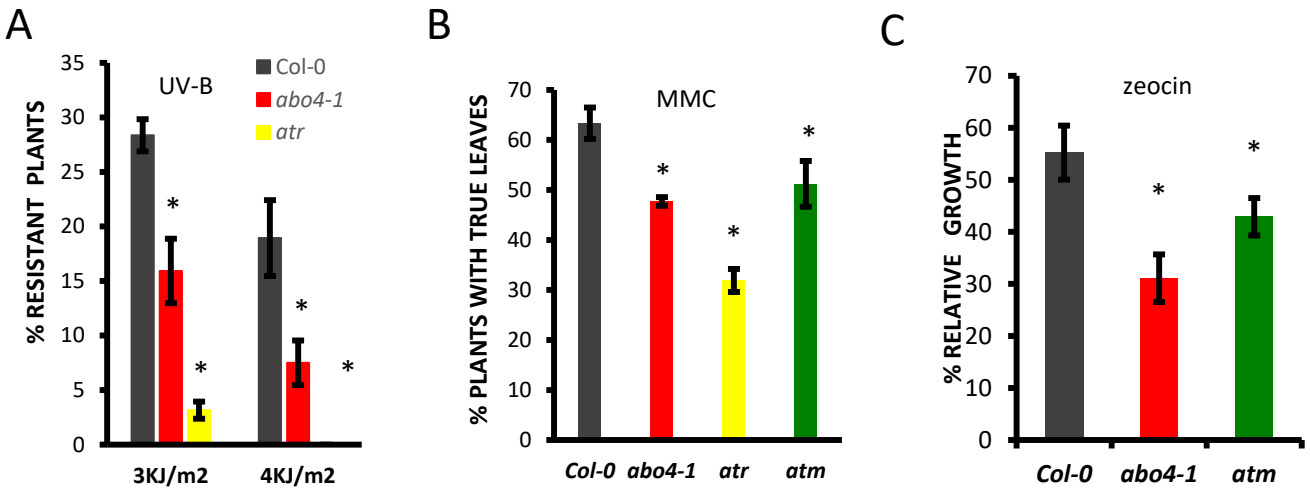

Figure S3. The *abo4-1* mutant is hypersensitive to genotoxic stress.
Wild-type (Col-0) and *abo4-1* seedlings were challenged with UV-B (A) mitomycin C (10 µM, B) and zeocin (10 µM, F). All these treatments induce not only replication blocking lesions but also DNA damage. The tolerance of seedlings to these genotoxic stresses were monitored as previously described (Pedroza-Garcia et al, 2016). The *atr* and *atm* mutants that are hypersensitive to these genotoxic agents were used as a positive controls. For all graphs, values are average +/- s.e. of three biological replicates and asterisks indicate statistically significant differences compared to the wild-type (student t-test, p value < 0.05).

A

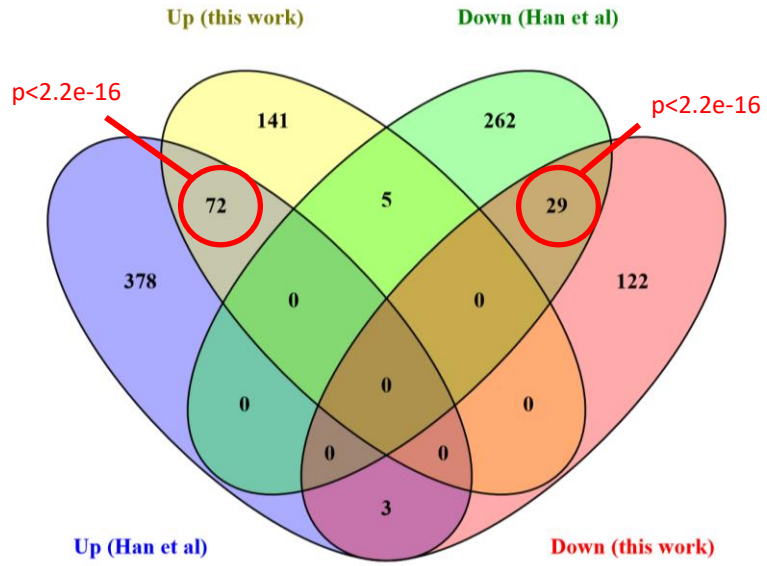

B

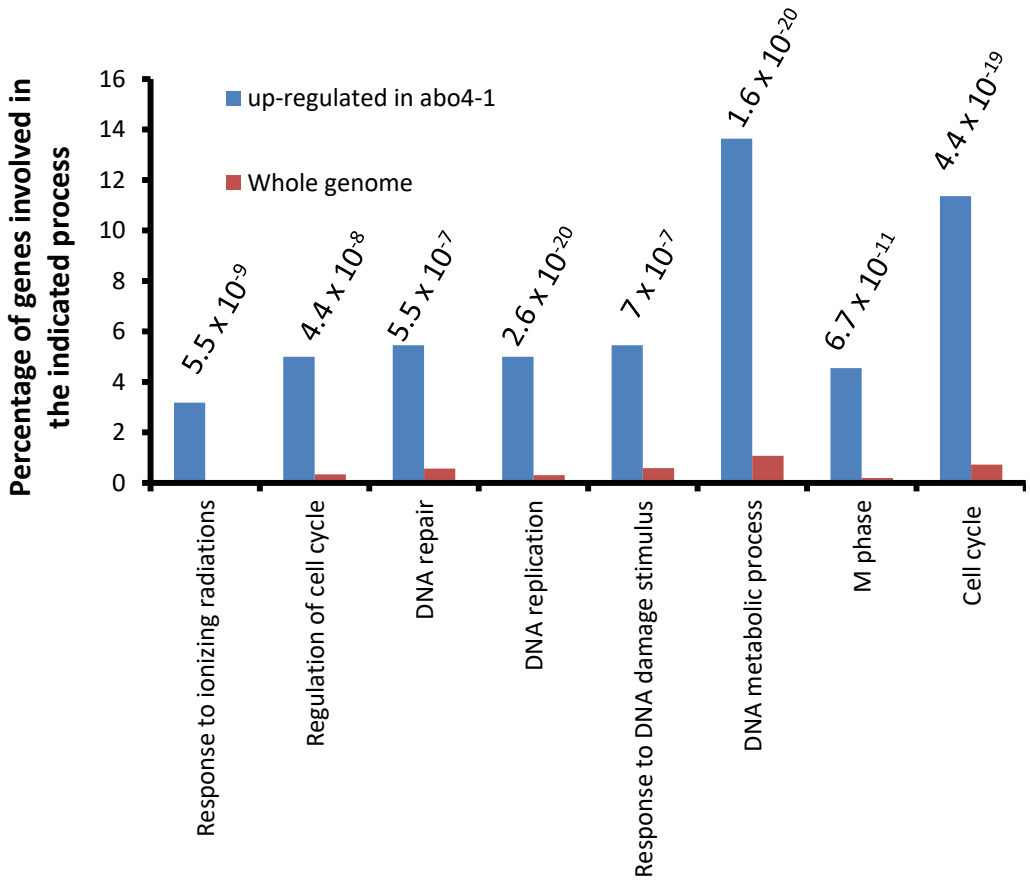

Figure S4: GO analysis of significantly induced genes in *abo4-1* seedlings.
A: Comparison between our RNAseq data and results published by Han et al (2015). Overlap between the two datasets is significantly higher than expected at random, although the majority of misregulated genes are identified in only one of the datasets. Genes found to be up-regulated in both datasets are all related to DNA repair, cell cycle or chromatin organization.
B: GO analysis was performed using the GO enrichment analysis tool (geneontology.org/page/go-enrichment-analysis). Values above bars indicate the p value associated with the enrichment (Bonferroni corrected).

Figure S5: The *sog1* mutation significantly reduces vegetative growth of the *abo4-1* mutant but partially rescues the *abo4-2* mutant.
Plants were grown in vitro for 10 days, and subsequently transferred to soil and grown in a green house for one month.

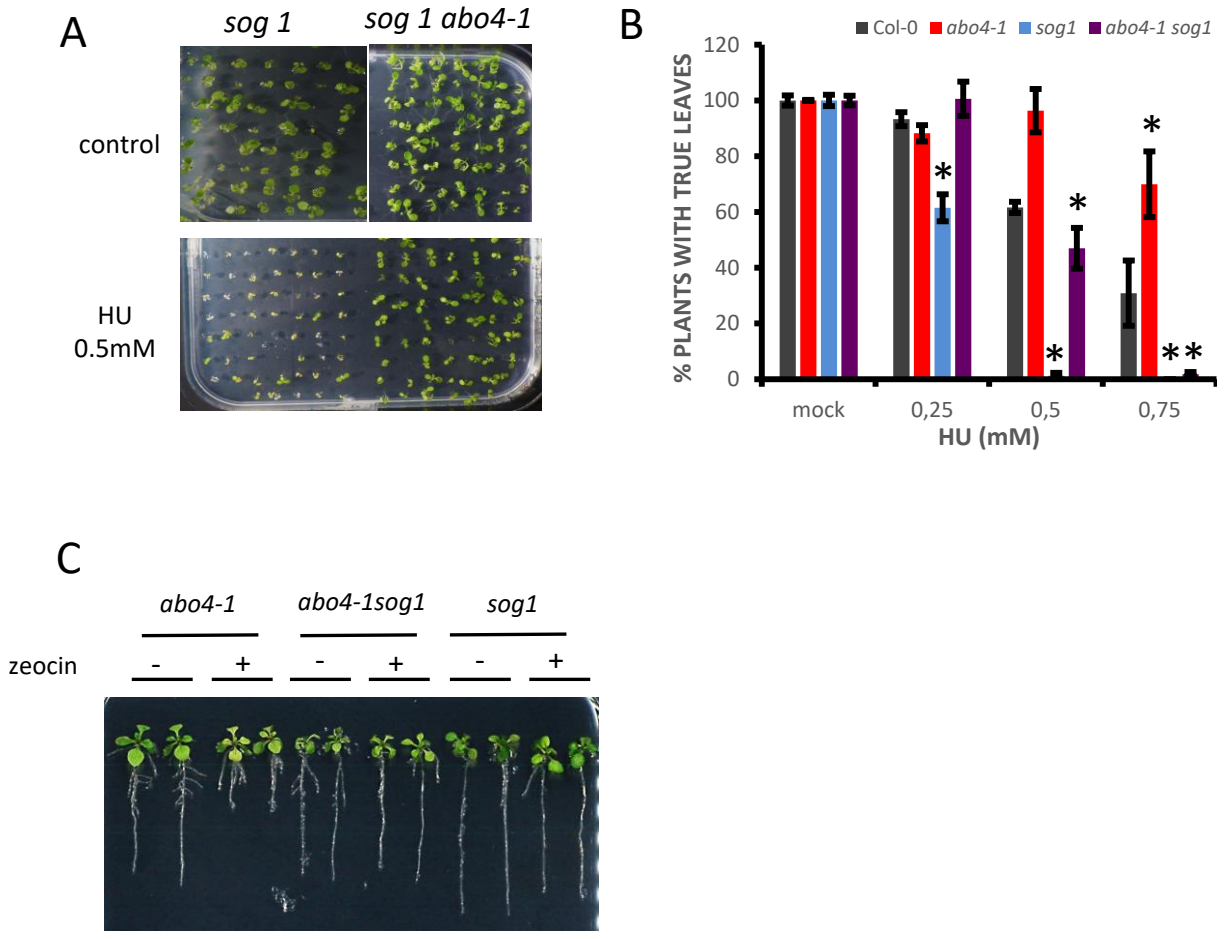

Figure S6: The SOG1 transcription factor is partly responsible for the tolerance of *abo4-1* mutants to HU and their sensitivity to zeocin.

A-B: Wild-type (Col-0) and *abo4-1, sog1 and abo4-1sog1* seedlings were germinated on half strength MS supplemented with HU to the indicated concentration. After 12 days, the percentage of plants with true leaves was monitored.

C: Representative phenotype of *abo4-1*, *sog1* and *abo4-1 sog1* plantlets 8 days after transfer to zeocin containing medium (10µM). The *sog1* mutant is completely resistant to zeocin, whereas the *abo4-1* mutant is highly sensitive, and the double mutant displays an intermediate phenotype.

For all graphs, values are average +/- s.e. and asterisks indicate statistically significant differences compared to the wild-type (student t-test p value < 0.05). Data are representative of at least 2 independent experiments.

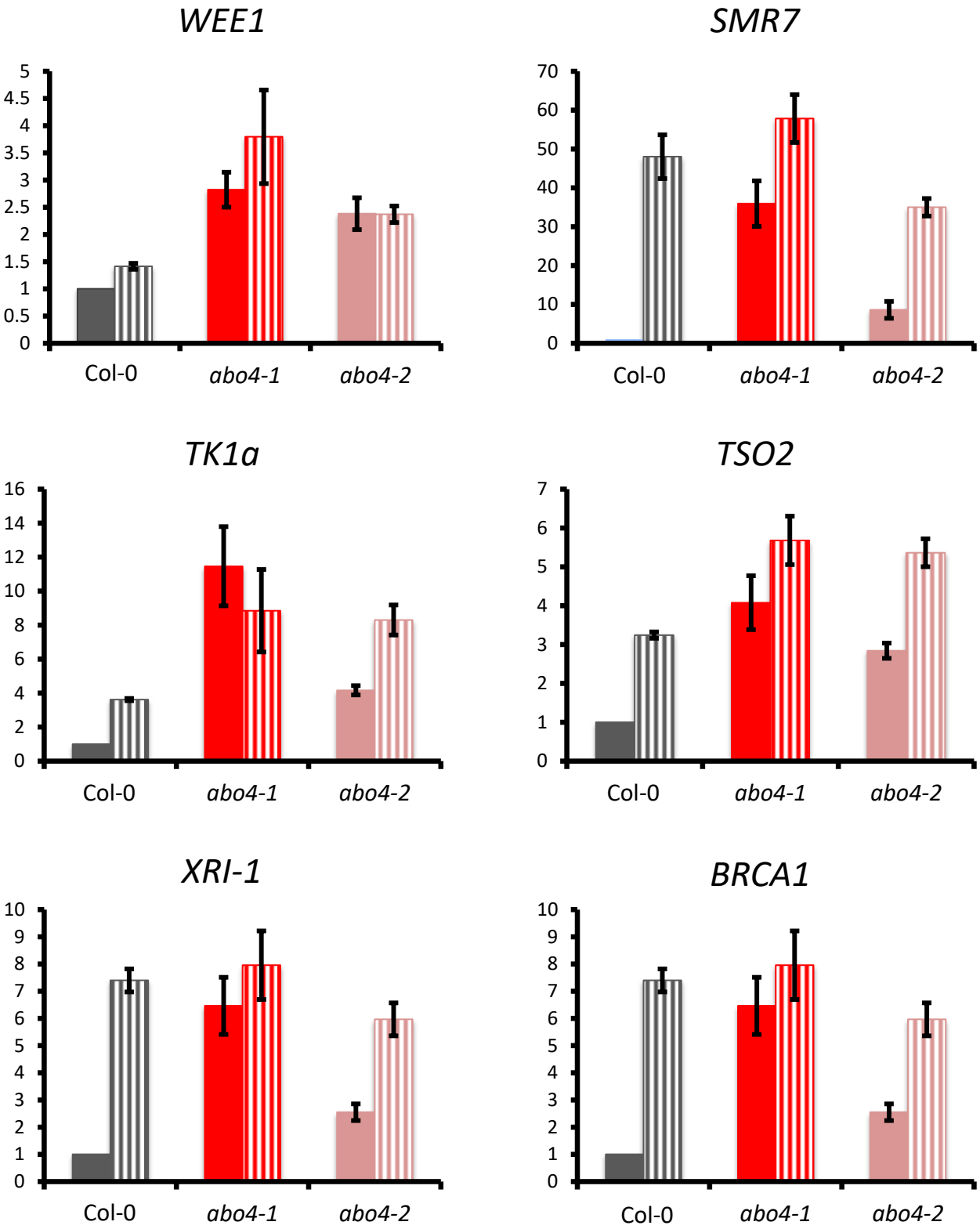

Figure S7: Transcriptional response to zeocin in *abo4* mutants.
qRT-PCR quantification of DDR genes expression in plantlets of the wild-type (Col-0), *abo4-1* and *abo4-2*, grown on control medium (full bars) or exposed to zeocin (10µM) for 24h (dashed bars). Values are expressed relative to the wild-type (Col-0). For all panels results are representative of two independent experiments.

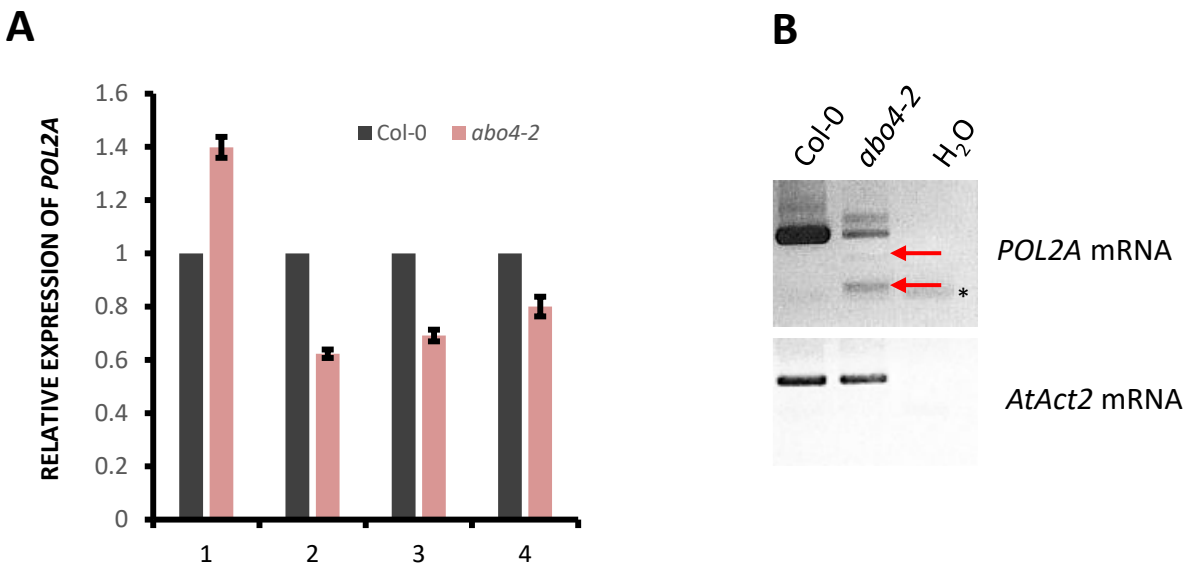

Figure S8: The T-DNA insertion in the *abo4-2* mutant leads to production of different variants of the *POL2A* mRNA.

A: All regions of the *POL2A* mRNA are accumulated in the *abo4-2* mutant. qRT-PCR quantification of POL2A mRNA accumulation. Primer pair 1 is situated upstream of the T-DNA insertion, pairs 2, 3 and 4 are situated downstream. The mutant shows slight hyper-accumulation of the 5' moiety of the POL2A mRNA, and some reduction in the accumulation of its 3' part. B: RT-PCR amplification pattern obtained with primers situated on both sides of the T-DNA insertion (in exons 11 and 14). Some cleanly spliced transcript can be amplified, and its sequence was confirmed to be identical to the wild-type. Additional PCR products of lower molecular weight can also be observed (indicated by red arrows), sequence analysis revealed that they result from alternative splicing events leading to the elimination of exon 12 (corresponding to amino acids 427 to 481) or exons 12 and 13 (corresponding to amino-acids 427 to 540). The asterisk indicates the position of an aspecific band present in the water control.

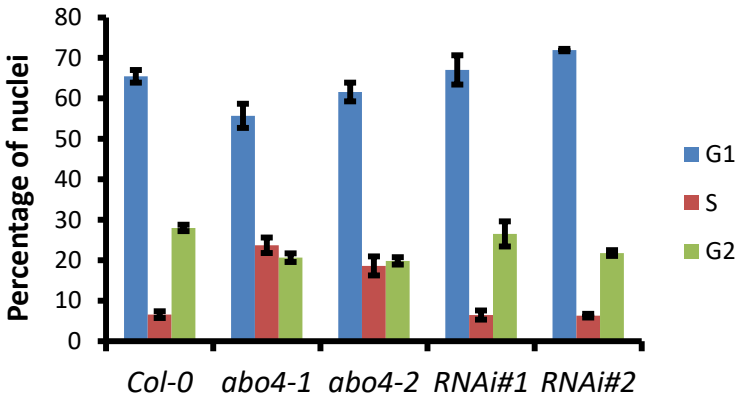

Figure S9: Partial inactivation and down-regulation of POL2A have contrasting effects on cell cycle regulation.

Distribution of flower buds nuclei between the G1, S and G2 phases of the cell cycle. *abo4-1* and *abo4-2* mutants show a significant increase in the number of S phase cells whereas RNAi lines are comparable to the wild-type.

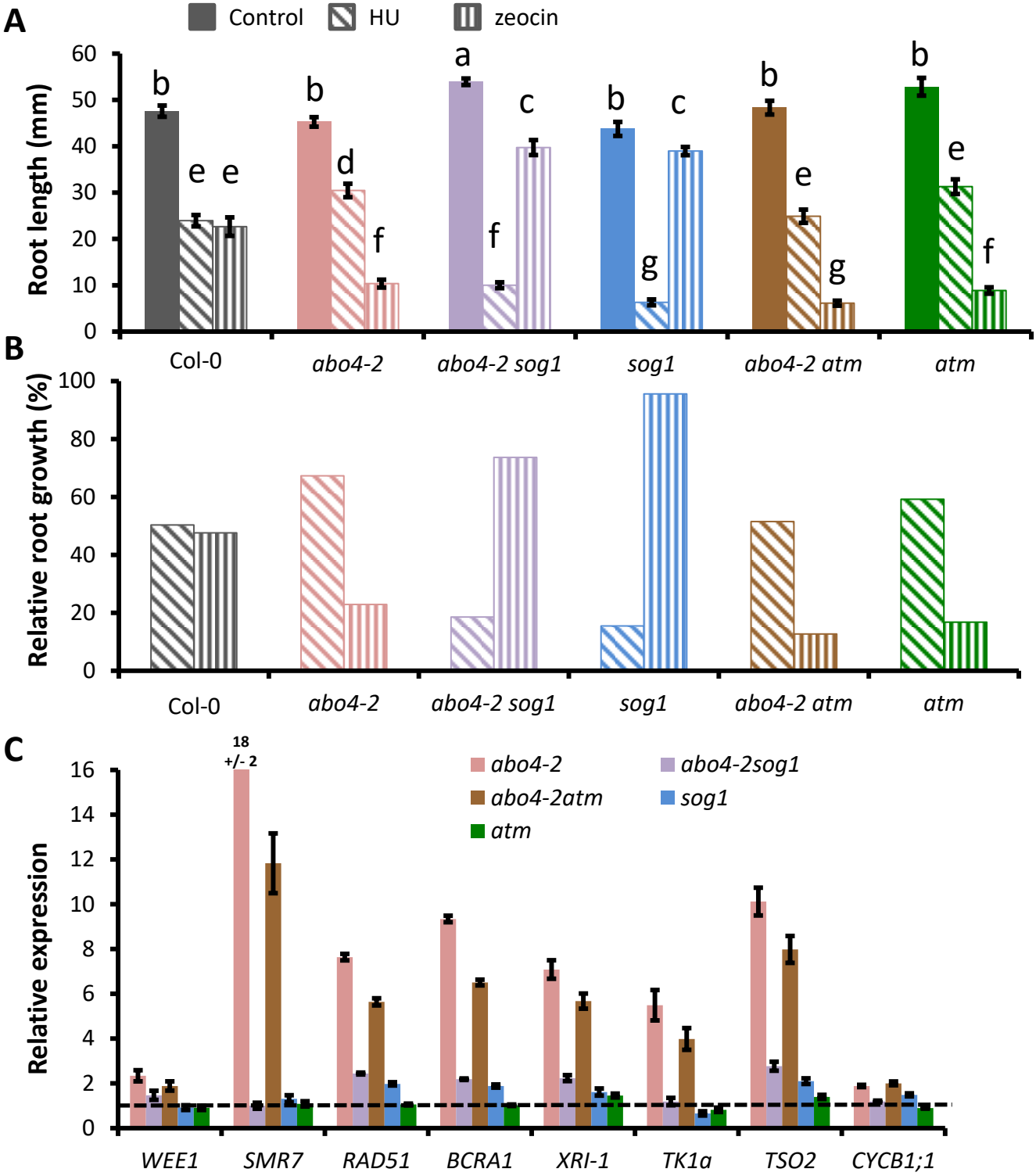

Figure S10: The *abo4-2* mutation confers HU tolerance that is partly dependent on SOG1.
A: Root length of wild-type (Col-0), *abo4-2*, *abo4-2 sog1*, *sog1*, *abo4-2 atm* and *atm* mutants after 9 days on control medium, or medium supplemented with HU (1mM) or zeocin (10µM). Values are average +/- s.e. Different letters above bars indicate statistically significant differences (Student t-test $p<0.05$). B: Relative root growth of wild-type (Col-0), *abo4-2*, *sog1*, *abo4-2 atm* and *atm* mutants after 11 days on HU (1mM) or zeocin (10µM). C: qRT-PCR quantification of DDR genes expression in flower buds of the *abo4-2*, *abo4-2 sog1*, *sog1 abo4-2 atm and atm* mutants. Values are expressed relative to the wild-type (Col-0). For all panels results are representative of two independent experiments.

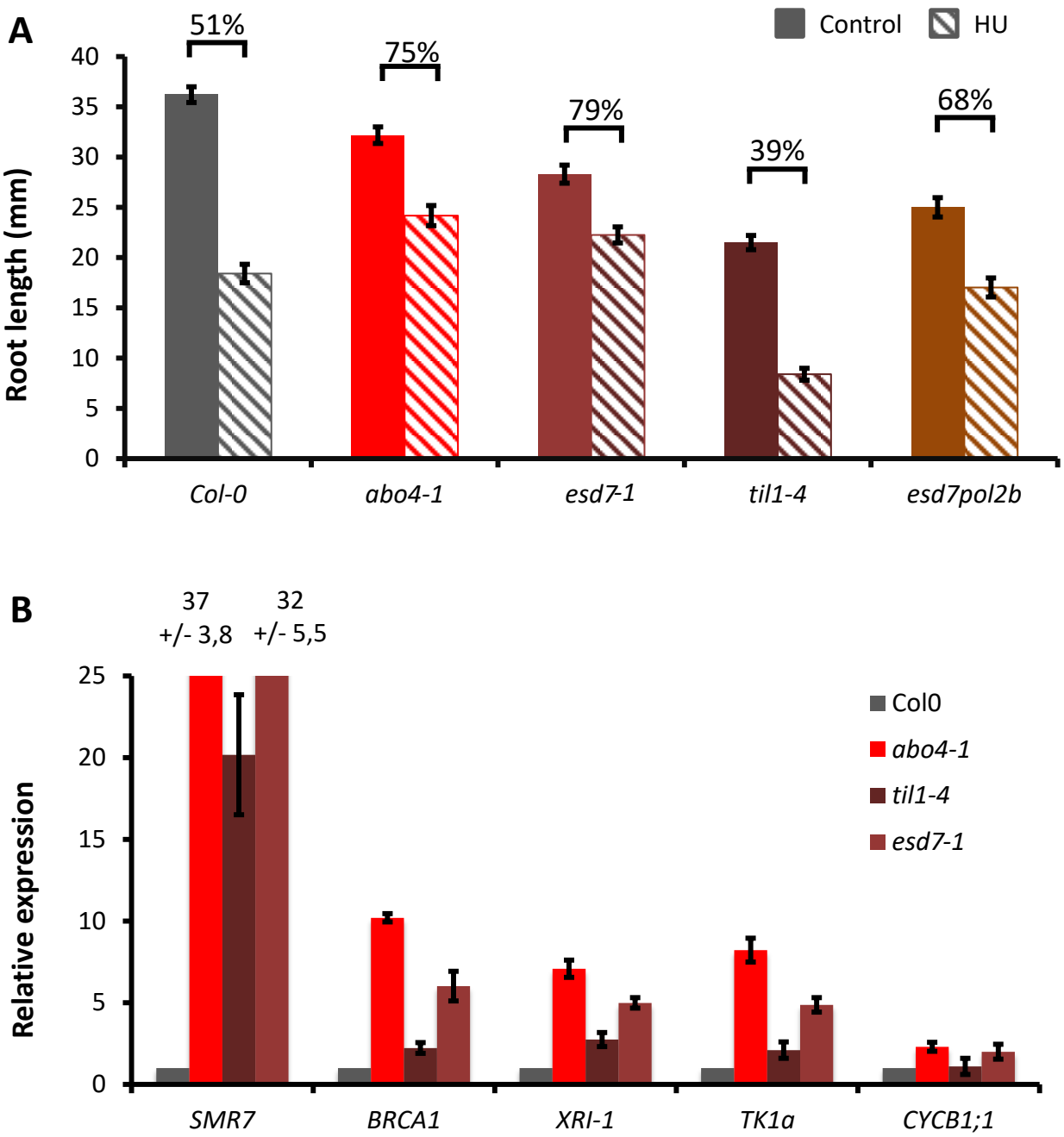

Figure S11: Different mutations in *POL2A* confer tolerance or hypersensitivity to replicative stress.

A: HU sensitivity in wild-type (Col-0), *abo4-1* and *esd7-1* (the *esd7-1* allele was introgressed into the Col-0 background for this experiment), *til1-4* mutants and *esd7-1 pol2b* double mutants. Plantlets were grown on half strength MS for 4 days and transferred to control medium (full bars) or HU supplemented medium (1mM, dashed bars) for 9 days. Values are average +/- s.e. obtained on at least 15 plantlets; values above bars indicate the relative growth observed on HU supplemented medium compared to control medium.

B: qRT-PCR quantification of DDR genes expression in plantlets of the *abo4-1*, *til1-4 and esd7-1* mutants. Values are expressed relative to the wild-type (Col-0). For all panels results are representative of two independent experiments.

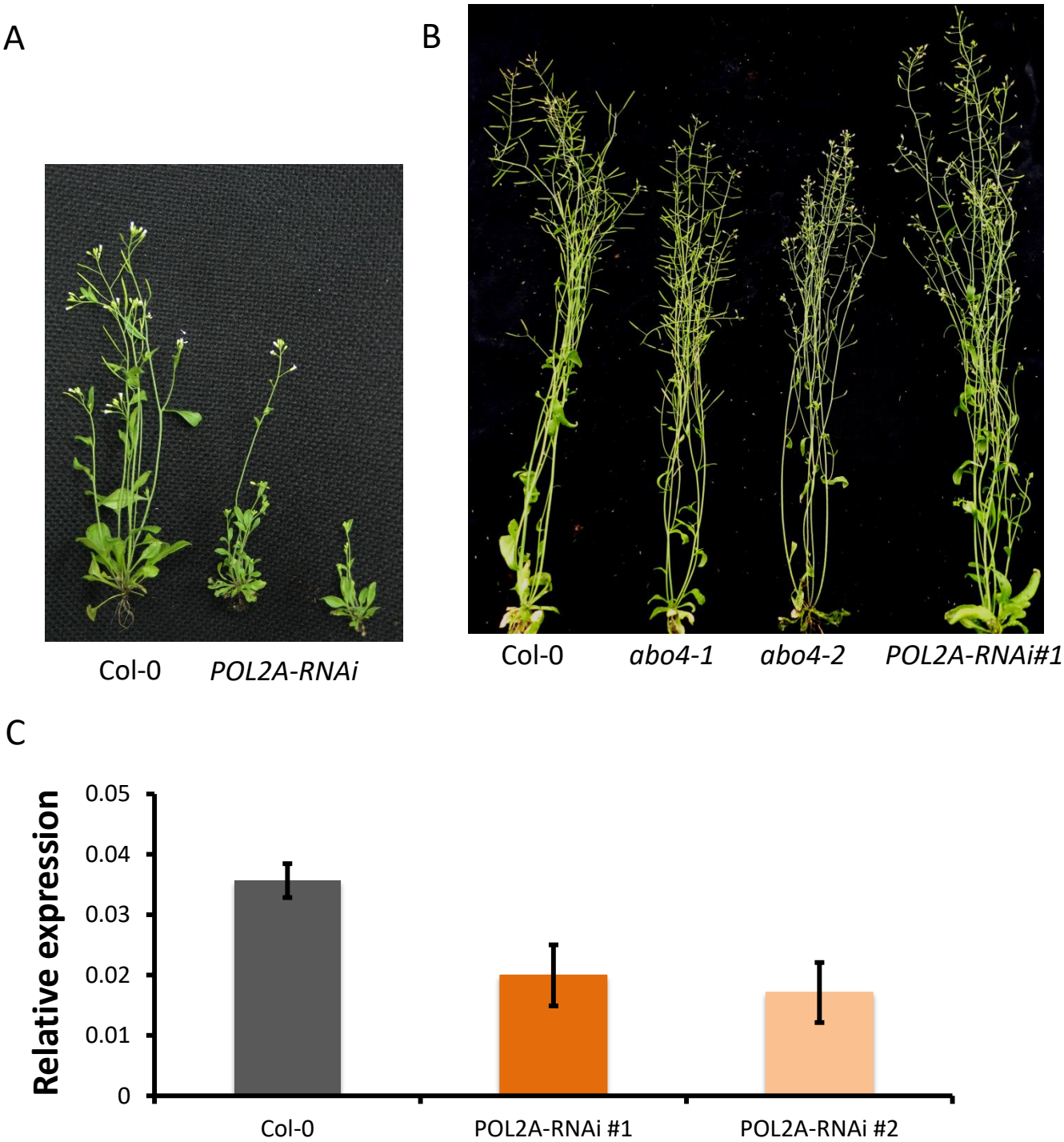

Figure S12: Down-regulation of *POL2A* affects plant growth and fertility.
A: examples of severe phenotypes obtained in several *POL2A-RNAi* lines.
B: phenotype of adult wild-type (Col-0), *abo4-1*, *abo4-2* and *POL2A-RNAi #1*. POL2A-RNAi lines used for further analysis reach the same size as wild-type plants but show a severe reduction in fertility.
C: qPCR quantification of *POL2A* expression in the two RNAi lines. *POL2A* expression was normalized with respect to *UBC21* expression. Values are average +/- SD.

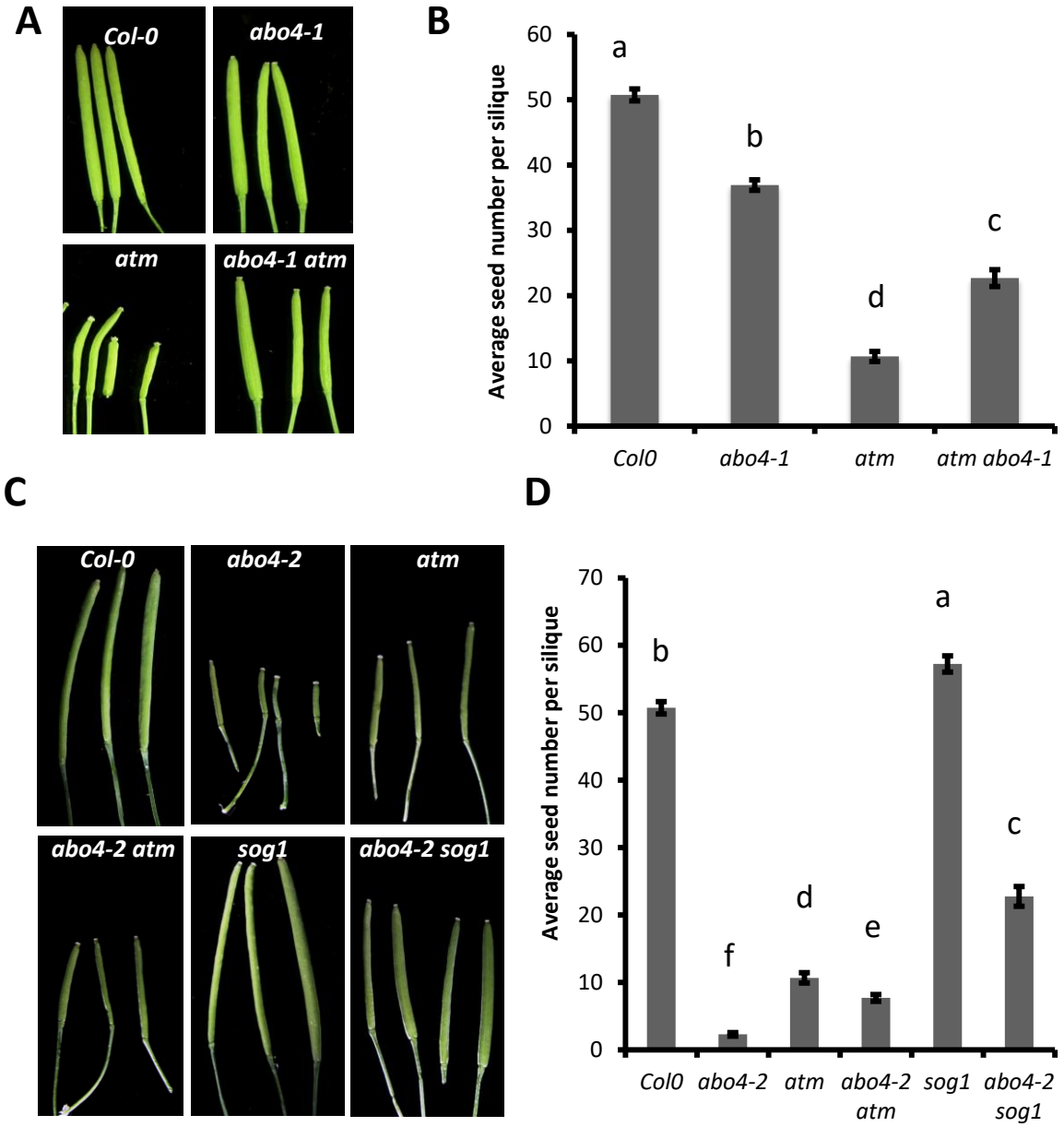

Figure S13: Genetic interactions between Pol ε and DDR genes during reproductive development.

A,B: The *abo4-1* mutation partially restores the fertility of atm mutants. A: representative pictures of siliques of wild-type (Col0), *abo4-1*, *atm* and *abo4-1 atm* mutants. B: Average seed number in siliques of the different genotypes. Values are average +/- s.e. of at least 20 siliques.

C,D: The *abo4-2* mutant is almost completely sterile, and these defects are partially rescued by the *sog1* mutation, and to a lesser extent by the *atm* mutation. C: representative pictures of siliques of the indicated genotypes, D: average seed number per silique in the different mutants, values are average +/- s.e. of data obtained in at least 20 siliques. In B and D, different letters indicate statistically significant differences (Student t-text $p<0.05$).

Table S1: Cell cycle length is drastically modified in *abo4* mutants but only mildly in *POL2-RNAi* lines.

	Col-0	*abo4-1*	*abo4-2*	*POL2A-RNAi 1*	*POL2A-RNAi 2*
Cell Cycle length (h)	19	32	32	21	22
S-phase length (h)	4	11	12	6	6
S-phase lenghth (%)	21	34	37	29	27

Table S3: List of genes involved in cell cycle, DNA repair, mitosis or meiosis that are up-regulated in *abo4-1*.

Cell cycle and DNA damage response

Locus	Description	fold change
AT1G02970	WEE1	2,4
AT3G27630	SIAMESE-RELATED 7	21,6
AT3G01330	DEL3 (DP-E2F-like 3)	2,2
AT1G76310	CYCLIN B2;4	1,7
AT4G37490	CYCLIN B1;1	2,2
AT2G17620	CYCLIN B2;1	2,4
AT2G26760	CYCLIN B1;4	1,8
AT2G38620	CDKB1;2	2,4
AT1G76540	CDKB2;1	1,9
AT3G54180	CDKB1;1	2,2
AT4G19130	REPLICATION PROTEIN A 1E, RPA1E	3,5
AT5G61000	REPLICATION PROTEIN A 1D	2,4
AT5G45400	REPLICATION PROTEIN A 1C, RPA1C	1,9
AT5G66130	RAD17	2,2
AT1G20750	RAD3-like DNA-binding helicase protein	8,1
AT5G20850	RAD51	3,7
AT3G19210	RAD54	2,5
AT4G21070	Breast cancer susceptibility1	4,8
AT1G04020	BARD1 (BREAST CANCER ASSOCIATED RING 1)	2,1
AT1G09815	"DNA polymerase delta subunit 4 family"	1,8
AT1G08260	POL2A catalityc subunit of Pol ε	1,5
AT3G07800	TK1a; Thymidine kinase	7,1
AT2G21790	RNR; RNR large subunit	2,1
AT3G27060	TSO2; RNR subunit	7,1
AT4G02390	Poly(ADP-Rib) polymerase	6,1
AT5G24280	΄ϒ-Irradiation and mitomycin c induced 1	5,8
AT5G48720	X-ray induced transcript 1	4,8
AT5G03780	TRF-like 10	4,0
AT4G03130	BRCT domain-containing DNA repair protein	3,0
AT3G52115	GR1; GAMMA RESPONSE 1	2,4
AT5G64060	ANAC103 ; transcription factor	4,5
AT2G42260	UVI4 (POLYCHOME, UV-B-INSENSITIVE 4)	2,1
AT2G18600	RUB1-conjugating enzyme, putative	2,5
AT3G27640	"transducin family protein / WD-40 repeat family protein"	1,9
AT1G02670	helicase-related	2,3
AT5G49110	unknown protein	2,9
AT4G24610	unknown protein;	1,8
AT5G48020	2-oxoglutarate (2OG)	1,7
AT5G13060	armadillo domain-containing protein	2,0
AT3G60840	microtubule associated protein (MAP65/ASE1)	2,0
AT3G03130	unknown protein	1,8
AT1G72670	IQD8; calmodulin binding	1,8
AT1G48605	"ATHAL3B (Hal3-like protein B); electron carrier"	2,9
AT3G25100	CDC45	2,1

Mitosis/Meiosis

Locus	Description	fold change
AT4G29170	ATMND1	2,6
AT5G52290	XPF endonuclease-like	2,8
AT3G27730	RCK (ROCK-N-ROLLERS)	2,3
AT1G53490	HEI10: Required for class I crossover .	3,5
AT5G40840	SYN2 (Sister chromatid cohesion 1 (SCC1)	2,3
AT1G06660	JASON	1,9
AT1G51130	Nse4, Smc5/6 DNA repair complex	2,2
AT1G49910	mitotic checkpoint protein,	2,3
AT3G42860	zinc knuckle (CCHC-type) family protein	2,1
AT3G59550	SYN3 (Sister chromatid cohesion 1 protein 3	1,9
AT3G57860	UV-B-INSENSITIVE 4-LIKE	1,9
AT4G15890	mitotic chromosome condensation	2,0
AT2G46980	ASY3	2,0
AT1G34355	PS1 (Parallel Spindle 1)	1,8
AT3G44050	"kinesin motor protein-related"	1,7

Table S4: Primers used in this study.

qPCR primers			
Gene	Accession Number		Sequence 5'->3'
RNR1	AT2G21790	Forward	GCTTAGCAGTGACCATTGTG’
		Reverse	TCAGCAGCCAACTCATCATCAAG
TSO2	AT3G27060	Forward	TCGCTTGTCTACTCTACACG
		Reverse	CCGCGTCGCAGACGATTGA
SMR7	AT3G27630	Forward	GCCAAAACATCGATTCGGGCTTC
		Reverse	TCGCCGTGGGAGTGATACAAAT
PARP2	AT2G31320	Forward	AGCCTGAAGGCCCGGGTAACA
		Reverse	GCTGTCTCAGTTTTGGCTGCCG
TK1a	AT3G07800	Forward	TTGGAAGATTCTGACAAGGCTA
		Reverse	CAACATTAAGGATAAACCAGACCA
CYCB1-1	AT4G37490	Forward	GGAAGCAACAAGAAGAAGGGAG
		Reverse	AGGGATCAAAGCCACAGCG
XRI1	AT5G48720	Forward	GCTACCTGATGACTTAAACTTTGGTTC
		Reverse	CATTTGGAGAAGATCGAGTCACAG
WEE1	AT1G02970	Forward	GGCCATTCGTTGCAGTTACA
		Reverse	TCTCGACATCTGAGAGACTC
BRCA1	AT4G21070	Forward	AGGTGAACCTGTCTCTGCGGATTT
		Reverse	TTCTCCGGCTTCTTGTCAACTCCA
RNR2A	AT3G23580	Forward	TGGCTCAGAACCAGAGATTC
		Reverse	AGAAACTGGCTTCAGCCTTC
UBC21	AT5G25760	Forward	CTGCGACTCAGGGAATCTTCTAA
		Reverse	TTGTGCCATTGAATTGAACCC
POL2A	AT1G08260	Forward	TCGCGATACTGGGAAAGTCT
		Reverse	TATCGGCGTCTCAAGTAGGC
PP2A3	AT1G13320	Forward	TAACGTGGCCAAAATGATGC
		Reverse	GTTCTCCACAACCGCTTGGT